

Lupanine and cytosine derivatives as antivirals: theoretical comparison on influenza, parainfluenza and SARS-CoV-2 viruses

Daniel I. Hădăruță^{1,*}, Nicoleta G. Hădăruță²

¹ Department of Applied Chemistry, Organic and Natural Compounds Engineering, Polytechnic University of Timișoara, 300001-Timișoara, Carol Telbisz 6, România

² Department of Food Science, Banat's University of Agricultural Sciences and Veterinary Medicine "King Michael I of Romania" from Timișoara, 300645-Timișoara, Calea Aradului 119, România

Abstract

The goal of the study was to evaluate the structural characteristics of some lupanine and cytosine derivatives against various viruses, i.e. influenza A virus subtype H1N1 (AH1N1), human parainfluenza virus type 3 (hPIV3) and the most recent severe acute respiratory syndrome coronavirus 2 (SARS-CoV-2), which determined the coronavirus disease 2019 pandemic (COVID-19). The molecular modelling, conformational analysis, quantitative structure-activity relationships (QSAR) and molecular docking techniques have been used. Nine lupanine or cytosine derivatives and two reference antivirals were studied by molecular modelling and conformational analysis using *MM+* molecular mechanics. A wide range of molecular descriptors were calculated for the most stable conformers using *QSAR Properties* and *PaDEL Descriptor* software. QSAR models with good statistical parameters were obtained for the largest absolute eigenvalue of Burden modified matrix - n_6 / weighted by relative Sanderson electronegativities (*SpMax6_Bhe*, correlation coefficient, $r = 0.62$) in the case of AH1N1 and for the information content index - neighborhood symmetry of 4-order (*IC4*, $r = 0.65$) in the case of hPIV3. The most active lupanine or cytosine derivative, (1*R*,5*R*)-9,11-dibromo-8-oxo-*N*-phenyl-1,5,6,8-tetrahydro-2*H*-1,5-methanopyrido[1,2-*a*][1,5]diazocine-3(4*H*)-carboxamide, having $pIC_{50} = 4.52$ against AH1N1 (antiviral activity close to the reference compound ribavirin, $pIC_{50} = 4.51$), was evaluated for its interaction capacity with AH1N1 and SARS-CoV-2 polymerase or protease. In both cases, the calculated interaction energies were favorable, indicating the possible increasing the antiviral activities by structural focusing on new quinolizidine based derivatives.

Keywords: AH1N1, hPIV3, SARS-CoV-2, COVID-19, QSAR, molecular docking, *Lupinus* species, lupanine derivatives, quinolizidine derivatives

1. Introduction

Lupin is the common name for *Lupinus* species. More than 200 species are known, some of them being valuable for human food and animal feed, mainly as legumes [1]. On the other hand, the presence of some biologically active secondary metabolites such as quinolizidine alkaloids opened the researches on biological activities of various semi-synthetic or synthetic derivatives [2-6]. (-)-Lupanine, (1*R*,2*S*,9*R*,10*R*)-7,15-diazatetracyclo[7.7.1.0^{2,7}.0^{10,15}]]heptadecan-6-one (mainly from *L. albus* L. and *L. angustifolius* L.) and (-)-cytosine, (1*R*,9*S*)-

7,11-diazatricyclo[7.3.1.0^{2,7}]trideca-2,4-dien-6-one (from *Laburnum* and *Cytisus* species) (Figure 1) are two alkaloids with moderate toxicities [4,7]. The structural modifications can reduce these toxicities and provide valuable biological activities such as antiviral properties [5,6].

Lupanine and cytosine derivatives were obtained by modifying/opening the A- and D-rings of (-)-lupanine or by substituting the A-ring and the N11 position of (-)-cytosine [6]. The main substituents were chloro, bromo, nitro on the A-ring and alkenyl-, cycloalkyl- or aryl-carbamoyl on the N11 of (-)-cytosine, which increased the antiviral activity.

* Corresponding author: daniel.hadaruga@upt.ro



Figure 1. Chemical structures of the natural (-)-lupanine and (-)-cytisine

Table 1. Structures of (-)-lupanine and (-)-cytisine derivatives and their biological activities against AH1N1 and hPIV3 viruses (activity expressed as pIC_{50} , where IC_{50} stands for 50 % inhibition of the viruses neuraminidase activity), as well as structures of the reference antiviral drugs, ribavirin and rimantadine (antiviral activities from [6])

Code	Structure	$pIC_{50(AH1N1)}$	$pIC_{50(hPIV3)}$
	R^3 R^5 R^{11}		
1	H NO ₂ Allyl	2.98	3.80
2	Br H Phenyl	4.23	3.89
3	H Br Adamantyl	3.61	5.52
4	Br Br Allyl	4.37	5.40
5	Br Br Phenyl	4.52	4.44
6	Br Br Adamantyl	3.20	4.49
7	Cl H Allyl	2.97	3.79
8	Cl H Phenyl	3.02	3.30
9	Cl H Adamantyl	3.37	4.60

Ribavirin
 $pIC_{50(AH1N1)} = 4.51$; $pIC_{50(hPIV3)} = 4.96$

Rimantadine
 $pIC_{50(AH1N1)} = 4.21$

These compounds are active against various viruses, including AH1N1 and hPIV3 strains [5,6]. H1N1 subtypes generates some of modern influenza pandemics, such as Spanish flu pandemic in 1918-1920 or 2009 swine flu pandemic [8-10]. On the other hand, AH1N1 determines the typical seasonal flu [11]. On the contrary, hPIV viruses determines the human parainfluenza, which causes respiratory illness in children, but it has low risks [12-14]. Both are RNA viruses and their attachment to the host cell and replication involves two glycoproteins,

hemagglutinin and neuraminidase, as well as a RNA polymerase, respectively [8,11-14].

The goal of the study was to evaluate the structural characteristics of some (-)-lupanine and (-)-cytisine derivatives (Table 1) against AH1N1 and hPIV3 viruses through the QSAR approach. Another aspect was to elucidate the interaction efficiency of the most active derivatives with the main enzymes responsible for AH1N1 and SARS-CoV-2 virus replications.

2. Materials and Method

2.1. Selection of antiviral compounds

Nine structures resembling with (-)-lupanine and (-)-cytisine were synthesized and analyzed by Fedorova and co-workers [6]. Mainly, they have chloro, bromo and nitro groups on the A-ring as well as allyl-, phenyl- or adamantyl-carbamoyl groups attached to the N11 heteroatom at the core structure (Table 1). Antiviral activity was expressed as the inhibitory activity 50 % (IC_{50}) against the neuraminidases of AH1N1 and hPIV3 viruses (Table 1). As references, ribavirin and rimantadine were considered and included in analysis.

2.2. Molecular modelling, conformational analysis and molecular descriptor determination

Molecular modelling of the eleven antiviral compounds were performed using molecular mechanics $MM+$ program from the HyperChem 7.52 package [15]. The following parameters were setup: bond dipoles for the electrostatic potential, bonds, angles, torsion, non-bonded, electrostatic and hydrogen-bonded components for the force field, Polak Ribiere with conjugated gradient for the molecular mechanics optimization algorithm, 0.05 kcal/mol for the minimum RMS gradient (root mean square), *in vacuo* as the optimization environment. Conformational analysis was performed using *Conformational Search* module from HyperChem. All flexible bonds and rings were included in analysis, with the following parameters: eight simultaneously variations of torsion angles, variations of the flexible bonds and rings in the ranges of $\pm 60^\circ \div \pm 180^\circ$ and $\pm 30^\circ \div \pm 120^\circ$, respectively. Only those conformers having internal energy up to 4 kcal/mol higher than the minimum (the most stable conformer) were retained. The other parameters were the same such as for molecular modelling and the iteration/optimization limits and the number of the retained conformations were set at 500 and 20, respectively.

Two different programs were used for the determination of molecular descriptor values. First, the most stable conformers were used for the determinations of simple structural descriptors, i.e. molecular surface and volume, hydration energy, the logarithm of the octanol/water partition coefficient ($\log P$), refractivity and polarizability, using *QSAR Properties* from HyperChem [15]. On the other hand, more than 1400 molecular descriptors were determined for the same stable

conformers using *PaDEL Descriptor 2.21* program [16]. They belong to constitutional, autocorrelation, BCUT (Burden - CAS - University of Texas eigenvalues), Burden-Moreau, Crippen, topological, Wiener, 3D autocorrelation, gravity indices, moment of inertia, RDF (radial distribution function descriptors) and WHIM (Weighted Holistic Invariant Molecular) molecular descriptors.

2.3. Quantitative structure – activity relationships (QSAR)

QSAR models were obtained by linear regression analysis using Statistica 7.1 package. Only monoparametric models were considered (Eq. 1):

$$pIC_{50} = A(\pm errA) + B(\pm errB) \cdot P \quad (\text{Eq. 1})$$

where pIC_{50} stands for the antiviral activity, expressed as the $-\log IC_{50}$, with IC_{50} the inhibitory concentration 50% against AH1N1 or hPIV3 neuraminidase activity, A and B stand for equation coefficients, $errA$ and $errB$ stand for standard deviations for coefficients, while P indicates the molecular parameter determined above. The correlation coefficient, r , standard deviation for the equation, s , and F -Fischer value were used for evaluating the statistical quality of the QSAR models. The intercorrelation matrix allows selecting the most significant parameters for QSAR equations.

2.4. Molecular docking and interaction energy for antiviral compound and AH1N1 or SARS-CoV-2 enzymes

Molecular docking of the most active lupanine/cytisine derivatives into the receptor site of the virus enzymes responsible for attaching and replication (polymerase for AH1N1 and protease for SARS-CoV-2) were performed by $MM+$ optimization of the complex. The minimum energy conformers of the most active antivirals were oriented into the receptor site in the same way such as for the reference compounds from the corresponding complex determined by X-ray diffraction (available at the Protein Data Bank, <https://www.rcsb.org/> [11,17,18]). Reference compounds used for enzyme characterization were H7728, 5-[(2-chlorophenyl)methyl]-2-hydroxy-3-nitrobenzaldehyde, for AH1N1 and baicalein, 5,6,7-trihydroxy-2-phenyl-4H-1-benzopyran-4-one, for SARS-CoV-2. They were replaced by lupanine/cytisine derivatives at stable conformations, maintaining the corresponding H-bonding groups and hydrophobic interaction

moieties such as for reference compounds. Antiviral compound:enzyme complex optimization was performed with the same MM+ module, Polak Ribiere algorithm and a RMS of 0.05 kcal/mol. The interaction energy was determined as the difference between the sum of internal energies of components alone (antiviral compound and enzyme – polymerase or protease) and the energy of the optimized complex. The interaction energy values were only used for comparison.

3. Results and Discussion

Antiviral compounds derived from lupanine/cytisine structures have relatively rigid conformations, excepting the moieties from the N11 position of the core structure (see Table 1). Consequently, the number of flexible bonds were low. The most stable conformers have the N11 moiety oriented toward the quinolizidine part, as is observed for some compounds in Figure 1.

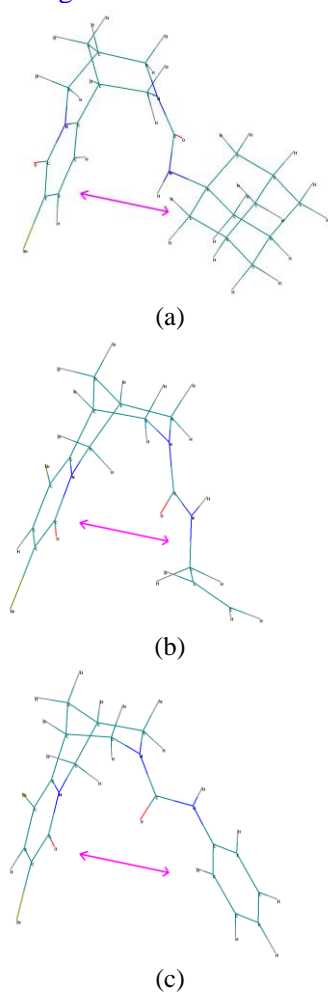


Figure 1. The most stable conformers of active compounds No 3, 4 and 5. Orientations of quinolizidine moiety and N11 substituents are indicated by pink arrows

There are variations among the significant parameter values, especially for the van der Waals molecular surface, hydrophobicity, as well as some constitutional (bond count), topological and information content descriptors. Thus, molecular surface has values in the range of 298-386 Å², with the minimum value for chloro and adamantyl based derivative No 9. Moreover, the hydrophobicity (*logP*) varies from -1.23 for compound No 1 to 0.62-0.67 for compounds No 3, 5 and 6. On the other hand, total double bonds descriptors have a wide variation from 3 to 7 and from 1 to 6 for *nBondsD* and *nBondsD2*, respectively. The standard compounds have the lowest values. The same observation can be done for *SpMax6_Bhe* and *IC4* descriptors, which have values of 2.89-3.12 and 4.77-5.15, respectively (Table 2). However, only *nBondsD2* intercorrelated with *SpMax6_Bhe* with a *r_{intercorr.}* of 0.79. This last parameter has no significant intercorrelation with the other *PaDEL* descriptors mentioned above (*r_{intercorr.}* of 0.45 with *nBondsD* and 0.47 with *IC4*).

Regarding the linear monoparametric models for both anti-AH1N1 and anti-hPIV3 using *QSAR Properties*, only molecular surface, *S(app)*, and the hydrophobicity, *LogP*, provide moderate results (Eqs. 2 and 3).

$$\begin{aligned}
 pIC_{50(AH1N1)} &= \\
 &= 5.42(\pm 1.20) - 0.0054(\pm 0.0038) \cdot S(app) \quad (\text{Eq. 2}) \\
 n &= 11, r = 0.428, s = 0.62, F = 2.02
 \end{aligned}$$

$$\begin{aligned}
 pIC_{50(hPIV3)} &= \\
 &= 4.24(\pm 0.24) - 0.279(\pm 0.173) \cdot \text{Log}P \quad (\text{Eq. 3}) \\
 n &= 10, r = 0.495, s = 0.67, F = 2.60
 \end{aligned}$$

Better correlations were obtained for *PaDEL* descriptors. Antiviral activity against AH1N1 has inverse correlations with both *nBondsD2* and *SpMax6_Bhe*, with correlation coefficients of 0.524 and 0.620, respectively (Eqs. 4 and 5). This suggests a less rigid molecule in the lupanine/cytisine derivative series for a higher antiviral activity.

Similar observations can be made for anti-hPIV3 activity, where *nBondsD* and *IC4* descriptors well correlates with this activity (*r* of 0.649 and 0.650, respectively, Eqs. 6 and 7).

Table 2. Values for the most significant molecular descriptors for anti-AH1N1 and anti-hPIV3 activities of lupanine/cytisine derivatives

Compound	$S(app)$ (Å ²)*	$LogP^{**}$	$nBondsD2^*$	$SpMax6_Bhe^*$	$nBondsD^{**}$	$IC4^{**}$
1	317.02	-1.23	6	3.13	6	5.11
2	323.97	0.45	4	2.90	7	5.15
3	329.48	0.62	4	3.12	4	4.77
4	327.73	0.31	5	2.89	5	5.02
5	348.86	0.63	4	2.92	7	5.15
6	386.05	0.67	4	3.12	4	4.81
7	323.54	0.59	5	2.89	5	5.02
8	343.83	0.36	4	2.92	7	5.15
9	298.32	0.22	4	3.12	4	4.77
Ribavirin	223.93	-2.06	1	2.54	3	4.77
Rimantadine	214.30	2.44	0	2.60	-	-

* Molecular descriptors that are significant for anti-AH1N1 activity

** Molecular descriptors that are significant for anti-hPIV3 activity

$$pIC_{50(AH1N1)} = 4.45(\pm 0.43) - 0.195(\pm 0.106) \cdot nBondsD2 \quad (\text{Eq. 4})$$

$n=11, r=0.524, s=0.58, F=3.40$

$$pIC_{50(AH1N1)} = 9.50(\pm 2.44) - 1.97(\pm 0.83) \cdot SpMax6_Bhe \quad (\text{Eq. 5})$$

$n=11, r=0.620, s=0.54, F=5.60$

$$pIC_{50(hPIV3)} = 6.09(\pm 0.72) - 0.32(\pm 0.13) \cdot nBondsD \quad (\text{Eq. 6})$$

$n=10, r=0.649, s=0.59, F=5.80$

$$pIC_{50(hPIV3)} = 18.31(\pm 5.75) - 2.79(\pm 1.16) \cdot IC4 \quad (\text{Eq. 7})$$

$n=10, r=0.650, s=0.59, F=5.80$

Taking into account these findings, the most active lupanine/cytisine derivatives at minimum energy conformations were subjected to molecular docking into the receptor sites of AH1N1 polymerase and SARS-CoV-2 protease. Equivalent groups and moieties of derivatives with the corresponding reference compounds, H7728 for AH1N1 (hydroxyl and carbonyl groups of H7728 and carbonyl group from A-ring of antiviral compounds, as well as chlorophenyl and phenyl moieties, respectively) and baicalein for SARS-CoV-2 (hydroxyl groups of baicalein and carbonyl group from A-ring of antiviral compounds, as well as phenyl moieties for

baicalein and corresponding antivirals), allowed favorable interactions between the antiviral compounds and specific enzymes. Best results were obtained for compound No 5, having two bromo groups on the A-ring and phenyl moiety at the N11 position of the core structure. All calculated interaction energies were positive, supporting the hypothesis that lupanine/cytisine derivatives can have favorable interactions with these virus enzymes and consequently to provide valuable antiviral activities. The optimized antiviral compound:enzyme complexes are presented in Figure 2.

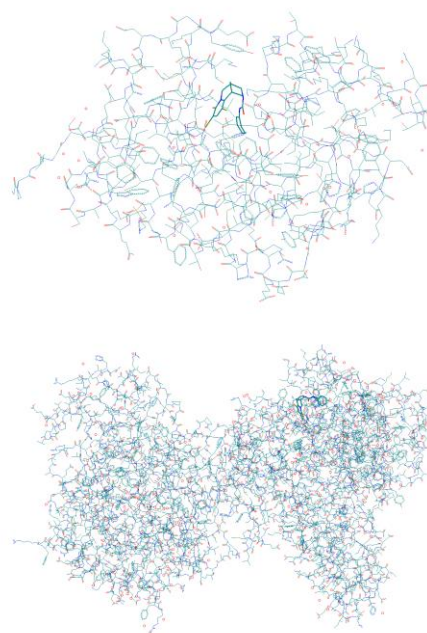


Figure 2. Optimized antiviral compound No 5:AH1N1 polymerase (top) and SARS-CoV-2 protease (bottom) complexes; lupanine/cytisine derivative No 5 was bolded

4. Conclusion

As a conclusion, molecular modeling, conformational analysis and the evaluation of QSAR models for nine lupanine/cytisine derivatives having inhibitory activity against influenza and parainfluenza viruses reveal the significance of the topological descriptors and the number of double bonds (which influence the molecular flexibility), as well as the informational content index for anti-influenza and anti-parainfluenza virus activity, respectively. Moreover, the interaction energies between some quinolizidine alkaloids and enzyme receptor sites showed positive values, indicating the efficiency in inhibiting the replication of these viruses and further focusing on new quinolizidine based derivatives as promising antivirals.

Acknowledgments. The author wants to thank S. Funar-Timofei and M. Mracec (“Coriolan Drăgulescu” Institute of Chemistry, Romanian Academy) for the help with Statistica 7.1 and HyperChem packages. The author also wants to thank C.M. Gabor for the contribution to molecular modeling of antivirals.

Compliance with Ethics Requirements. Authors declare that they respect the journal’s ethics requirements. Authors declare that they have no conflict of interest.

References

- [1] Wolko, B.; Clements, J.C.; Naganowska, B.; Nelson, M.N.; Yang, H., *Lupinus*. In: Cole, C. (ed.), *Wild Crop Relatives: Genomic and Breeding Resources, Legume Crops and Forages*, Springer-Verlag, Berlin Heidelberg, **2011**, pp. 153-206, https://doi.org/10.1007/978-3-642-14387-8_9
- [2] Carmali, S.; Alves, V.D.; Coelho, I.M.; Ferreira, L.M.; Lourenco, A.M., Recovery of lupanine from *Lupinus albus* L. leaching waters, *Separation and Purification Technology* **2010**, *74*, 38-43, <https://doi.org/10.1016/j.seppur.2010.05.005>
- [3] Magalhães, S.C.Q.; Fernandes, F.; Cabrita, A.R.J.; Fonseca, A.J.M.; Valentão, P.; Andrade, P.B., Alkaloids in the valorization of European *Lupinus* spp. seeds crop, *Industrial Crops and Products* **2017**, *95*, 286-295, <http://dx.doi.org/10.1016/j.indcrop.2016.10.033>
- [4] Wink, M., Quinolizidine Alkaloids: Biochemistry, Metabolism, and Function in Plants and Cell Suspension Cultures, *Planta medica* **1987**, *53*(6), 509-514, <https://doi.org/10.1055/s-2006-962797>
- [5] Rouden, J.; Lasne, M.-C.; Blanchet, J.; Baudoux, J., (-)-Cytisine and Derivatives: Synthesis, Reactivity, and Applications, *Chem. Rev.* **2014**, *114*, 712-778, <https://doi.org/10.1021/cr400307e>
- [6] Fedorova, V.A.; Kadyrova, R.A.; Slita, A.V.; Muryleva, A.A.; Petrova, P.R.; Kovalskaya, A.V.; Lobov, A.N.; Zileeva, Z.R.; Tsypyshev, D.O.; Borisevich, S.S.; Tsypysheva, I.P.; Vakhitova, J.V.; Zarubaev, V.V., Antiviral activity of amides and carboxamides of quinolizidine alkaloid (-)-cytisine against human influenza virus A (H1N1) and parainfluenza virus type 3, *Natural Products Research* **2019**, <https://doi.org/10.1080/14786419.2019.1696791>
- [7] Mohamed, A.A.; Rayas-Duarte, P., Composition of *Lupinus albus*, *Cereal Chemistry* **1995**, *72*(6), 643-647
- [8] Lin, T.; Wang, G.; Li, A.; Zhang, Q.; Wu, C.; Zhang, R.; Cai, Q.; Song, W.; Yuen, K.-Y., The hemagglutinin structure of an avian H1N1 influenza A virus, *Virology* **2009**, *392*, 73-81, <https://doi.org/10.1016/j.virol.2009.06.028>
- [9] Arora, R.; Chawla, R.; Marwah, R.; Arora, P.; Sharma, R.K.; Kaushik, V.; Goel, R.; Kaur, A.; Silambarasan, M.; Tripathi, R.P.; Bhardwaj, J.R., Potential of Complementary and Alternative Medicine in Preventive Management of Novel H1N1 Flu (Swine Flu) Pandemic: Thwarting Potential Disasters in the Bud, *Evidence-Based Complementary and Alternative Medicine* **2011**, 586506, <https://doi.org/10.1155/2011/586506>
- [10] de Jong, J.C.; Rimmelzwaan, G.F.; Fouchier, R.A.M.; Osterhaus, A.D.M.E., Influenza Virus: a Master of Metamo, *Journal of Infection* **2000**, *40*, 218-228, <https://doi.org/10.1053/jinf.2000.0652>
- [11] Fudo, S.; Yamamoto, N.; Nukaga, M.; Odagiri, T.; Tashiro, M.; Hoshino, T., Endonuclease inhibitor 1 bound to influenza strain H1N1 polymerase acidic subunit N-terminal region at pH 7.0, *PDB Protein Data Bank* **2015**, <https://doi.org/10.2210/pdb5FDD/pdb>
- [12] McLaughlin, L.P.; Lang, H.; Williams, E.; Wright, K.E.; Powell, A.; Cruz, C.R.; Colberg-Poley, A.M.; Barese, C.; Hanley, P.J.; Bollard, C.M.; Keller, M.D., Human parainfluenza virus-3 can be targeted by rapidly ex vivo expanded T lymphocytes, *Cytotherapy* **2016**, *18*, 1515-1524, <http://dx.doi.org/10.1016/j.jcyt.2016.08.010>
- [13] Li, Z.; Guo, D.; Qin, Y.; Chen, M., PI4KB on Inclusion Bodies Formed by ER Membrane Remodeling Facilitates Replication of Human Parainfluenza Virus Type 3, *Cell Reports* **2019**, *29*, 2229-2242, <https://doi.org/10.1016/j.celrep.2019.10.052>

- [14] Liu, Y.; Xie, W.; Chi, M.; Wen, H.; Zhao, L.; Song, Y.; Liu, N.; Chi, L.; Wang, Z., Mutations in the HRB linker of human parainfluenza virus type 3 fusion protein reveal its importance for fusion activity, *Virus Research* **2020**, 275, 197791, <https://doi.org/10.1016/j.virusres.2019.197791>
- [15] HyperChem, version 7.52, **2005**, Hypercube, Inc., Gainesville, FL, USA
- [16] Yap, C.W., PaDEL-Descriptor: An open source software to calculate molecular descriptors and fingerprints, *Journal of Computational Chemistry* **2011**, 32(7), 1466-1474
- [17] Su, H.X., Zhao, W.F., Li, M.J., Xie, H., Xu, Y.C., SARS-CoV-2 3CL protease (3CL pro) in complex with a novel inhibitor, *PDB Protein Data Bank* **2020**, <https://doi.org/10.2210/pdb6M2N/pdb>
- [18] Fudo, S.; Yamamoto, N.; Nukaga, M.; Odagiri, T.; Tashiro, M.; Hoshino, T., Two Distinctive Binding Modes of Endonuclease Inhibitors to the N-Terminal Region of Influenza Virus Polymerase Acidic Subunit, *Biochemistry* **2016**, 55, 2646-2660, <https://doi.org/10.1021/acs.biochem.5b01087>